

Western University

From the Selected Works of Anna Gunz

2020

Extreme heat and paediatric emergency department visits in Southwestern Ontario

Anna Gunz, *Western University*

Piotr Wilk, *University of Western Ontario*

Alana maltby

Tharsha Ravichakaravarthy

Kristin Clemens, et al.

Increased Insulin-like Growth Factor Binding Protein-I Phosphorylation in Decidualized Stromal Mesenchymal Cells in Human Intrauterine Growth Restriction Placentas

Sahil S. Singal, Karen Nygard, Robert Gratton, Thomas Jansson, and Madhulika B. Gupta 

Department of Biochemistry (SSS, MBG), Biotron (KN), Department of Obstetrics & Gynecology (RG), Department of Pediatrics (MBG), University of Western Ontario, London, Ontario, Canada; Department of Obstetrics & Gynecology, University of Colorado Anschutz Medical Campus, Aurora, Colorado (TJ); and Children's Health Research Institute, London, Ontario, Canada (MBG)

Summary

Intrauterine growth restriction (IUGR) is often caused by placental insufficiency, which is believed to be associated with decreased delivery of oxygen and nutrients to the placental barrier. We recently reported that hypoxia and/or leucine deprivation triggered hyperphosphorylation of insulin-like growth factor binding protein-I (IGFBP-I) in decidualized human immortalized endometrial stromal cells (HIESCs), resulting in decreased insulin-like growth factor-I (IGF-I) bioactivity. To test the hypothesis that human IUGR is associated with increased decidual IGFBP-I phosphorylation at discrete sites, we used IUGR and gestational age matched appropriate for gestational age (AGA) placentas ($n=5$ each). We performed dual immunofluorescence immunohistochemistry (IHC) using IGFBP-I and vimentin as decidual and mesenchymal markers, respectively. Employing a unique strategy with imaging software, we extracted signal intensity of IGFBP-I expressed specifically from truly decidualized cells of the placenta. Relative IGFBP-I was increased (85%; $p=0.0001$) and using custom phospho-site-specific antibodies, we found that IGFBP-I phosphorylation (pSer101; +40%, $p=0.0677$ /pSer119; +60%, $p=0.0064$ /pSer169; +100%, $p=0.0021$) was markedly enhanced in IUGR. Together, our data links for the first time, increased decidual IGFBP-I phosphorylation at discrete sites with human IUGR. These novel findings suggest that hyperphosphorylation of IGFBP-I in decidualized stromal mesenchymal decidual basal layer contributes to potentially elevated levels of phosphorylated IGFBP-I in maternal circulation in IUGR pregnancies. (J Histochem Cytochem 66:617–630, 2018)

Keywords

Alexa 568, Alexa 660, decidua basalis, dual immunofluorescence, fetal growth, gestational age, immunohistochemistry, quantitative image analysis, vimentin

Introduction

Intrauterine growth restriction (IUGR) increases perinatal morbidity and mortality¹ and predisposes for diabetes and cardiovascular disease later in life.² IUGR is often caused by placental insufficiency, which is believed to be associated with decreased delivery of oxygen and nutrients to the placental barrier. Impaired trophoblast invasion into the maternal decidua has been suggested to cause placental insufficiency leading to

IUGR.³ However, the molecular mechanisms underlying the development of IUGR are incompletely understood, no clinically useful biomarker for early detection

Received for publication July 28, 2017; accepted March 16, 2018.

Corresponding Author:

Madhulika B. Gupta, Children's Health Research Institute, VRL Room A5-136 (WC), 800 Commissioners Road E., London, ON, Canada N6C 2V5.
 E-mail: mbgupta@uwo.ca

is available, and there is currently no effective therapy for IUGR once diagnosed.

During pregnancy, insulin-like growth factors (IGFs) and IGF-binding proteins (IGFBPs) are important for the growth and differentiation of maternal, placental, and fetal tissues. IGFBP-1 is the predominant IGFBP in human amniotic fluid^{4,5} and a major IGFBP in fetal plasma.⁶ The main site of IGFBP-1 production during pregnancy is the fetal liver, which secretes IGFBP-1 into fetal circulation.⁷ IGFBP-1 is phosphorylated,^{8,9} and its phosphorylation uniquely increases IGFBP-1's affinity for IGF-1 and augments its capacity to inhibit the biological effects of IGF-1 in human fetal and placental growth.^{10–12} We previously showed that IGFBP-1 is hyperphosphorylated at specific sites in the cord blood of human IUGR infants and in the fetal liver from a baboon model of maternal nutrient restriction.¹³ Together, our previous findings suggest a novel mechanism of action whereby fetal liver IGF-1 bioavailability is markedly decreased by increased site-specific phosphorylation of IGFBP-1, strongly suggesting fetal IGFBP-1 hyperphosphorylation contributes to reduced fetal growth in human IUGR.¹⁴

The decidua plays a critical role in modulating maternal-fetal resource allocation. Decidual IGFBP-1 regulates the biological activity of IGF-1 within the local environment of the human placenta.⁵ IGFBP-1 expression is particularly high in the decidua of the basal plate (decidua basalis) and membranes,¹⁵ and IGFBP-1 is a recognized marker for decidual cells.¹⁶ Using a transgenic mouse model, decidual IGFBP-1 overexpression has been associated with altered placental development and impaired fetal growth.¹⁷

Phosphorylated IGFBP-1 isoforms are also present in the decidua.¹² However, the cellular localization of site-specific decidual IGFBP-1 phosphoisoforms is unknown and it remains to be established if the abundance of IGFBP-1 phosphorylation at distinct amino acid residues in the decidua is altered in IUGR pregnancies. Our recent findings of marked site-specific IGFBP-1 hyperphosphorylation in response to hypoxia and/or nutrient deprivation in cultured decidualized human immortalized endometrial stromal cells (HIESCs),¹⁸ is consistent with the possibility that decidual IGFBP-1 phosphorylation at Ser101, Ser119, and Ser169 (individually or in combination) is modulated in IUGR due to placental insufficiency.

The purpose of this study was to perform relative quantitation of IGFBP-1 phosphorylation in IUGR versus appropriate for gestational age (AGA) pregnancies, specifically from truly decidualized mesenchymal cells. To test the hypothesis that human IUGR is associated with increased decidual IGFBP-1 phosphorylation at

discrete sites, we performed traditional dual immunofluorescence immunohistochemistry (IHC). To determine relative levels of IGFBP-1 phosphorylation at Ser101, Ser119, and Ser169, we utilized a unique strategy with Image Pro Premier software, and selectively collected dual immunofluorescent signal intensity in vimentin positive decidual cells in placenta tissues from AGA and IUGR group ($n=5$ each; Fig. 1).

Materials and Methods

Selection of Study Subjects

Human placenta samples were collected through our ongoing collection for studies on IUGR.^{19–22} Pregnant women were recruited at London Health Sciences Centre (LHSC). Samples were collected under approval by the Western University Research Ethics Board. The infant/maternal clinical data were obtained from their medical records. Birth weight percentiles were calculated using standardized gender-specific growth charts. IUGR was defined as having a birth weight below the 10th percentile, while severe IUGR was a birth weight below the 3rd percentile. Four out of the five IUGR samples used were from infants with a birth weight <3rd percentile and with the presence of at least one sign of fetal compromise (such as low ponderal index, abnormal umbilical artery Doppler or oligohydramnios) as an additional criterion to minimize the risk of inclusion of constitutionally small fetuses. Mothers of IUGR pregnancies were otherwise healthy. Control subjects selected were women delivering a term infant with a birth weight for AGA defined as 25th to 75th percentile. Gestational age (GA) was determined by last menstrual period. Healthy controls were selected to match as closely as possible the GA range. We compared IUGR placenta (33–37 weeks gestation) matched with AGA controls ($n=5$ each). The samples selected for this cohort were matched for inclusion and exclusion criteria briefly as follows: Women with singleton pregnancies were included. Pregnancies with congenital abnormalities, diabetes, thyroid disorders, chronic hypertensive disorders or pre-eclampsia, premature rupture of membranes, placental abruption, fetal congenital and genetic abnormalities, chorioamnionitis, smokers, drug abuse, and malnutrition were excluded, as in our previous studies.^{19–22}

Tissue Collection

Placentas from IUGR and AGA pregnancies ($n=5$ each) were randomly selected from both vaginal and/or cesarean section and collected immediately after delivery. Based on review of the pathological reports

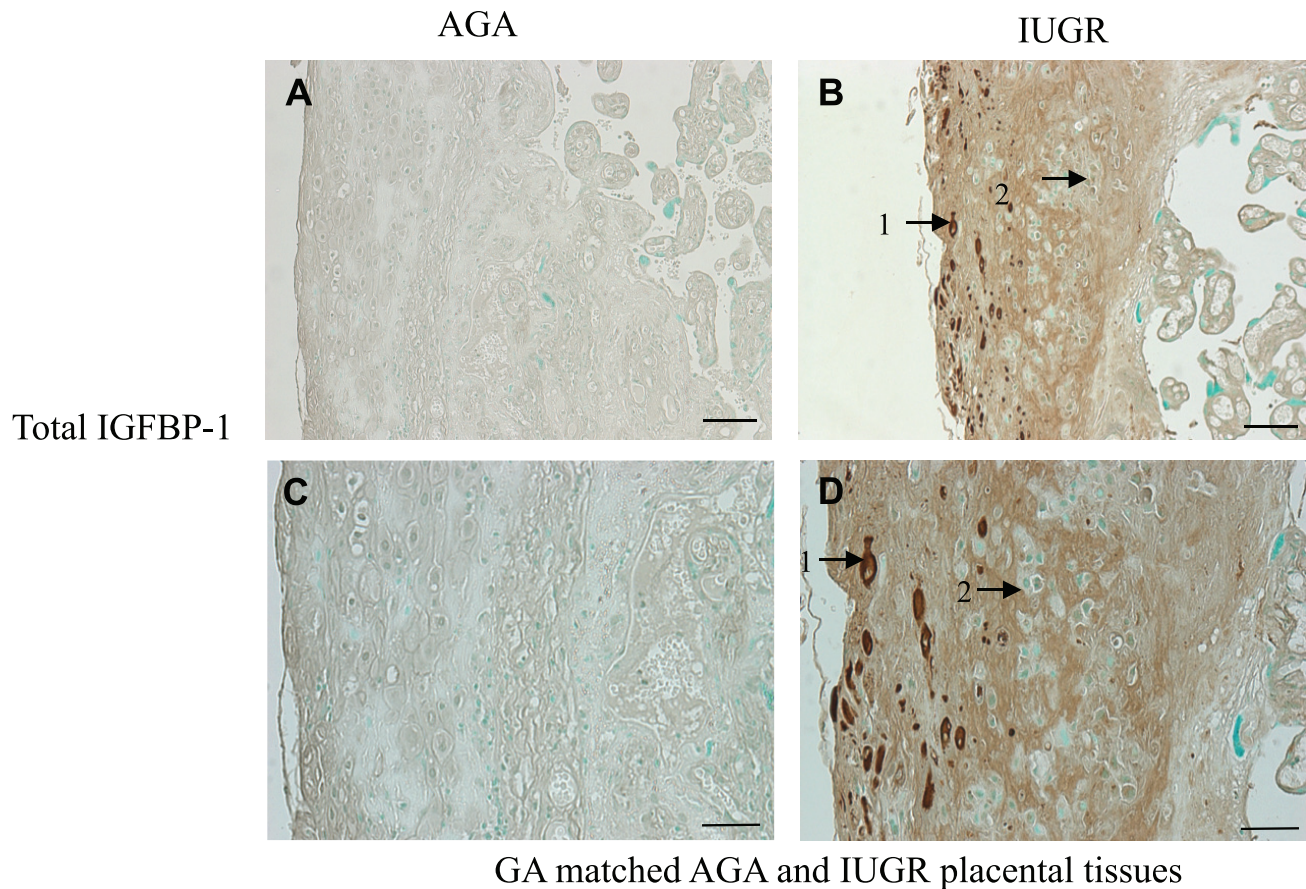


Figure 1. Decidual localization of IGFBP-1 abundance in AGA and IUGR placental tissues via immunohistochemistry. Immunostaining of IGFBP-1 in human term placenta from normal (AGA; A and C) and IUGR pregnancy (B and D) showing IGFBP-1 expression in basal plate decidual (Arrow-1) and cytotrophoblast (Arrow-2) cells. Intervillous space and fetal capillaries did not indicate any IGFBP-1 staining. Most of the decidual stromal cells in IUGR express higher levels of IGFBP-1 relative to GA-matched AGA placental tissues. Shown in (A) and (B) are 10× objective (scale bar = 50 μ M). (C) and (D) are 20× objective, scale bar = 100 μ M. Abbreviations: IGFBP-1, insulin-like growth factor binding protein-1; AGA, appropriate for gestational age; IUGR, intrauterine growth restriction; GA, gestational age.

(undertaken at the LHSC), all of the placentas were negative for signs of infection, and also contained no major infarcts. The tissue samples were collected and full thickness blocks were obtained. All tissues were sectioned serially (consistent thickness of 5 μ m; Biotron Integrated Microscopy Laboratory, The University of Western Ontario [UWO]) and mounted on pretreated slides (Superfrost Plus, Fisher Scientific, Fairlawn, NJ). The selection of regions within each block of the placenta was based on the criteria that ensured incorporating all levels/regions from chorionic plate to basal plate. GA-matched AGA and IUGR placenta tissues ($n=5$ each) were placed side-by-side on a slide and labeled as shown in Fig. 2A. Six representative images from each of the placental tissues ($n=5$ each) were captured (Fig. 2A, red squares and image represented in Fig. 2B) and used for dual immunofluorescence staining and image analysis as described further.

Sample Preparation

A stratified random sampling procedure was used. The decidua region was identified as the superficial layer on the maternal facing side of the placenta, to ensure regions were inclusive of decidual (basal plate decidua [BPD]) tissue for IHC as confirmed based on morphology through H&E staining. The sections were treated according to the standard immunofluorescent technique for detection of IGFBP-1 and vimentin.

Antibodies

The following primary antibodies were used: IGFBP-1 mAb 6303 (Catalog #0027301; Medix Biochemica, Kauniainen, Finland), mAb vimentin (Catalog #M7020; Dako, Burlington, Ontario, Canada). Pre-immune serum used as negative controls were Dako Mouse Immunoglobulin and Dako

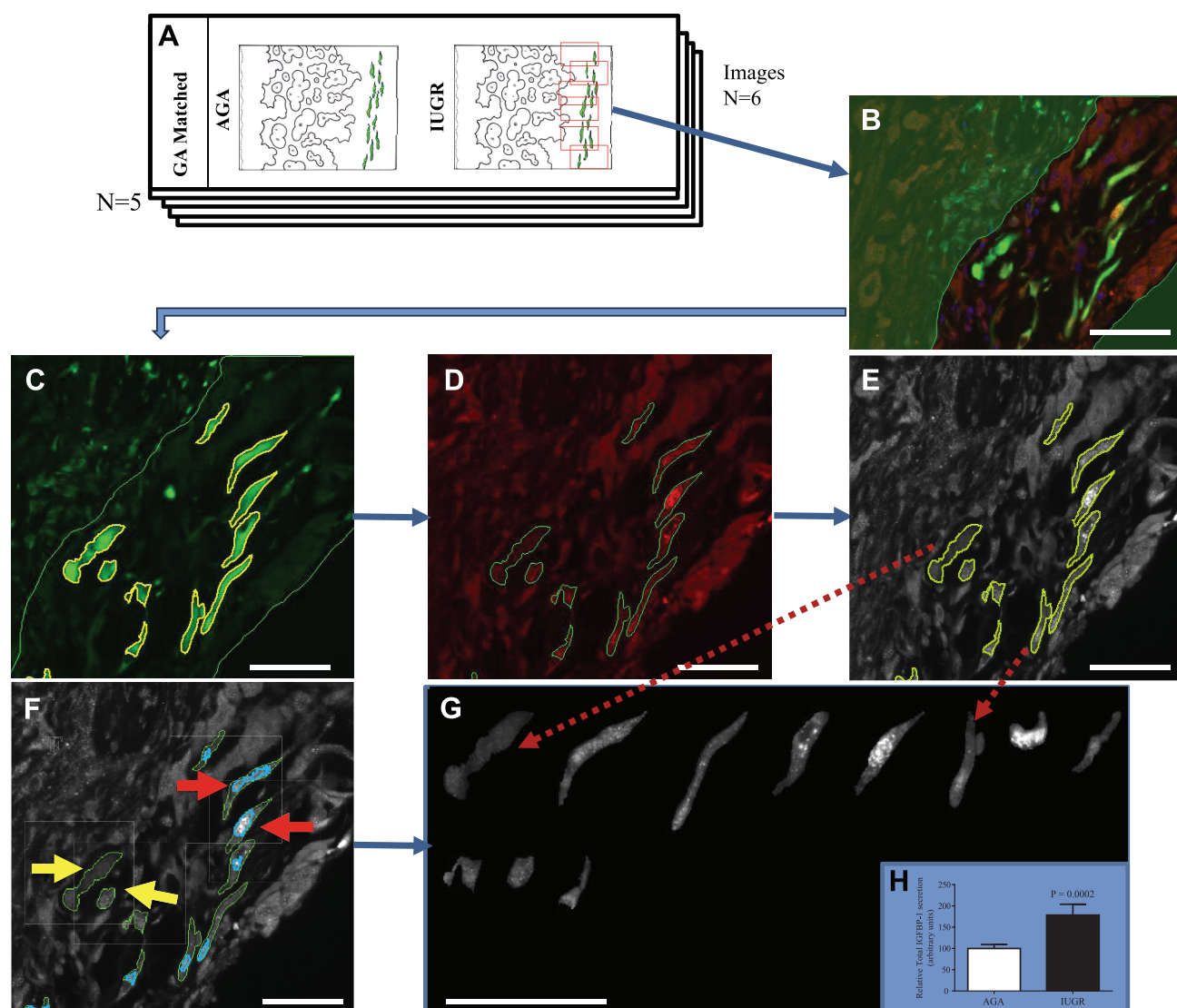


Figure 2. Flowchart showing experimental design and methodology for dual immunofluorescent staining and image analysis. Image Pro Premier software-based quantification, and statistical analysis. IUGR and matched AGA placenta ($n=5$) were stained simultaneously for vimentin, plus total, or phosphorylated (Ser 101, Ser 119, or Ser 169) IGFBP-1. Representative images ($n=6$ regions/sample-red outlines as shown) were captured as multichannel images from the BPD of each placenta tissue ($n=5$), using standardized microscope settings (A and B). A manual ROI was drawn to isolate the decidualized cells within the basal plate (C). Within this ROI on the Vimentin channel (Alexa 660-shown green), vimentin positive mesenchymal cells were counted to create cell outlines (C, D). Cell outlines from (C) were converted into multicell ROIs and applied onto the raw channel image from the matching total or phosphorylated (Ser 101, Ser 119, and Ser 169) IGFBP-1 image—Alexa 568-shown in (E) grayscale for better viewing. Within the cellular ROIs, high expressing cells only were counted, using IGFBP-1 signal itself to isolate truly decidualized cells (blue outlines, red arrows) from nondecidualized cells—green outlines, yellow arrows (F). A cell-sorted image was created to illustrate the intensity differences in signal between the IUGR and AGA. Matching cells dotted red arrows (between E and G). Data were generated from within the blue outlined, truly decidualized cell population in (E). Scale bar = 100 μ m. Abbreviations: IUGR, intrauterine growth restriction; AGA, appropriate for gestational age; IGFBP-1, insulin-like growth factor binding protein-1; BPD, basal plate deciduas; ROI, region of interest; GA, gestational age.

Rabbit Immunoglobulin Fraction (Normal) each. We used our prevalidated custom made IGFBP-1 polyclonal antibodies targeting pSer101, pSer119, and pSer169^{13,23} (generated at YenZyme Antibodies

LLC, San Francisco, CA). Secondary antibodies were antirabbit Alexa 568 (Catalog #A11036) and antimouse Alexa 660 (Catalog #A21055; ThermoFisher, Waltham, MA).

Immunohistochemistry

The tissue sections were incubated for 10 min in 3% H₂O₂ to quench endogenous peroxidase. After a 2 × 5 min PBS wash, endogenous Biotin was blocked using an Avidin-Biotin blocking kit. Briefly, avidin solution was applied for 10 min, rinsed in PBS, followed by biotin solution for 10 min, to prevent reagent avidin molecules from adhering to the endogenous biotin known to be present in placental tissues. After a brief rinse with PBS, tissues were blocked using Dako Background Sniper (Biocare Medical, Concord, CA) for 10 min. They were rinsed with PBS and IGFBP-1 (mAb 6303) as primary antibody (1:10,000; 100 µL) was applied for overnight incubation at 4°C, using pre-immune serum as a negative control. All incubations were performed in a humidified chamber. Next, Vectastain Elite kit biotinylated secondary antibody matching the primary host (Vector Laboratories, Burlington, ON, Canada; 1:200) was applied for 45 min at room temperature followed by Vectastain Elite Avidin-biotin peroxidase complex for a further 45 min. Next, 3,3'-Diaminobenzidine (DAB) staining was performed for 2 min per slide with Cardassian DAB (Biocare Medical, Concord, CA). For counterstaining, tissues sections were stained with methyl green (Vector Laboratories, Burlington, ON, Canada) pre-heated to 60°C for 5 min and the slides were dehydrated, cleared in xylene and mounted with Permount (Fisher Scientific, Burlington, ON, Canada).

Dual Immunofluorescence

After deparaffinization and following blocking and a PBS wash, the slides were incubated with a mixed 120 µL solution of primary antibodies; vimentin plus IGFBP-1 antibody or vimentin plus individual phospho-site-specific IGFBP-1 antibodies (pSer101, pSer119, and pSer169) for 1 hr. The dilutions for the antibodies were Vimentin (1:25), rabbit polyclonal IGFBP-1 (1:10,000), and each of the phospho-site-specific IGFBP-1 antibodies (pSer101, pSer119, and pSer169; 1:1000). Pre-immune serum was used as a negative control. Combinational secondary antibodies (100 µL), Alexa 568 (polyclonal antirabbit) and Alexa 660 (monoclonal antimouse; 1:400) were added and incubated at room temperature for 1 hr. The tissues were then counterstained with 100 µL of 4',6-Diamidino-2-Phenylindole, Dihydrochloride (DAPI; Life Technologies, Burlington, ON, Canada) for 2 min with a 1:200 dilution, rinsed in PBS, mounted with Prolong Gold Mounting Media (Life Technologies, Burlington, ON, Canada) and sealed with nail polish.

Selection of Placental Regions and Image Standardization and Acquisition

Axiolmager Z1 Epifluorescent Microscope and Zen Pro software (Carl Zeiss Canada Ltd, Toronto, ON, Canada) was utilized to capture images using a 20 × objective. The fluorescent lamp was preheated for 15 min prior to imaging to stabilize lamp intensity. For image uniformity, camera settings were then set to avoid saturation and autofluorescent background, and consistently applied at the same settings for all imaging.

Representative images ($n=6$) from each of the dually stained placenta tissues from AGA and IUGR group ($n=5$ each; represented in Fig. 2A), stained with vimentin plus one of total IGFBP-1 or IGFBP-1 phosphorylation at Ser101, Ser119 and Ser169 (Fig. 2A and B) were acquired within the BPD regions (Fig. 2A, red squares, $n=6$ each, and image represented in Fig. 2B). This allowed coverage of large areas for each placenta, which subsequently provided an adequately large number of cells/image to represent per cell data to quantitate our results.

Quantitative Image Pro Software Analysis

Threshold Setting. To quantify the relative immunofluorescent signal intensities of total and IGFBP-1 phosphorylation at Ser101, Ser119, Ser169 specifically in decidual cells, we used Image Pro Premier 9.2 software (Media Cybernetics, Rockville, MD). A detailed strategy (flowchart) of Image Pro analysis is described in Fig. 2A-H and in Supplemental Fig. 1. To isolate the expression of IGFBP-1 specifically in decidual cells versus whole, multicellular BPD region, we set a threshold using IGFBP-1 itself. Threshold settings were tested on various slides to check for cells with consistent decidual morphological characteristics, and on negative controls to ensure specificity. Utilizing Image Pro software feature for imaging and quantitation specifically based on accounting for precise cell-by-cell basis, we aimed for counting a minimum of 100 cells per placenta.

Defining the Truly Decidualized Cells From the Overall Mesenchymal Cell Population. First, to define mesenchymal decidua, regions of interest (ROIs) outlines were drawn manually around the BPD region and applied to the vimentin (pseudo-green/Alexa 660) channel image (Fig. 2C). Cells within this ROI that were positively stained with vimentin were selected based on signal intensity thresholds to create mesenchymal cell outlines within the basal plate (Fig. 2C and D). The software

then stored the geographical location of these outlines, and applied them onto the matching total IGFBP-1 or phosphorylated IGFBP-1 (pSer101/pSer119/pSer169) channel images (Fig. 2D and E). We subsequently applied a second binary threshold within these mesenchymal cell outlines to measure only the subpopulation of decidualized mesenchymal cells, to more precisely collect our data only from highly IGFBP-1 expressing cells (Fig. 2F). These sequential steps allowed us to define and select the truly decidualized cells from the overall mesenchymal cell population.

Cell Sorted Images and Quantification. In addition, to demonstrate the changes in overall IGFBP-1 signal intensity/strength in the vimentin positive cells, the underlying IGFBP-1 signal was then cropped from the image, recreated, and resorted in grayscale (Fig. 2G). These sequential steps led us to define and select the truly decidualized cells from the overall mesenchymal cell population to visualize signals more effectively when removed from the surrounding tissue. The mean intensity of total IGFBP-1 or phosphorylated IGFBP-1 (pSer101/pSer119/pSer169) within these decidualized mesenchymal cells was then recorded (Fig. 2H) from AGA and IUGR pregnancies. A flowchart of Image Pro analysis is also described in (Supplemental Fig. 2A–C).

Data Presentation and Statistical Analysis

Statistics were performed using GraphPad Prism 5 (Graph Pad Software Inc., CA). Dual immunofluorescent images captured from six different regions of each placental tissue section from AGA and IUGR were used to quantify the mean intensity for each placenta. We then calculated the average of the mean intensities across the samples (Fig. 2A) and compared the intensities of total and phosphorylated IGFBP-1 (pSer101/pSer119/pSer169), respectively, in AGA and IUGR placental tissues ($n=5$ each). The mean intensity of the control (AGA) was assigned an arbitrary value of 100. All mean values for IUGR were expressed relative to this mean. To compare means, unpaired Student's *t*-test was performed, and the results were expressed as mean \pm SEM with $n=5$ samples. Significance was accepted at $p<0.05$.

Results

Clinical Characteristics

The clinical characteristics of the AGA and IUGR pregnancies included in this study are as follows: The

mean maternal age in the AGA group was 36 ± 4.58 compared with 31.80 ± 2.78 years in the IUGR group, with no significant differences. Mean GAs were similar, with 34.8 ± 0.97 and 35.6 ± 0.68 weeks in AGA and IUGR, respectively. Cesarean section and vaginal deliveries were included in both groups. The mean placental weight was 449 ± 66.87 and 386 ± 36.01 grams in the AGA and IUGR groups, respectively. The mean birth weight for IUGR infants (1812 ± 194 grams) was significantly lower than AGA (2323 ± 28 grams) and so were the birth weight percentiles, which were 28.75 and 2.80 for AGA and IUGR, respectively ($p<0.05$). The other clinical data did not show significant differences between study groups. All IUGR newborns ($n=5$) were confirmed to be growth restricted with birth weight <3rd percentile except for one at 7th percentile.

Relatively Higher Abundance of IGFBP-1 in Decidual Cells of Placenta

We first aimed to immunohistochemically (Biotin-Avidin staining) localize decidual cells in the placenta tissue sections (Fig. 1). The decidua basalis or the basal plate, which is the maternal part of the placenta, forms an important contact between maternal and fetal tissue where the decidual marker IGFBP-1 is localized.¹⁵ We located the basal plate region in tissue sections based on overall morphology and vimentin positive staining. Maternal decidual cells of the basal plate region, which were identified by immunoreactivity to vimentin (not shown), expressed IGFBP-1 in high abundance (Fig. 1B–D, Arrow-1). Based on the signal intensity using equal exposure criteria, as expected, IGFBP-1 was expressed in most decidual cells of the basal plate but in variable abundance (Fig. 1B and D). The maternal side of villus parenchyma includes a thin basal plate corresponding to the maternofetal junction made up of trophoblasts, stromal, and fibroblast-like cells. Most of the staining for IGFBP-1 was observed in stromal-like decidual cells (Fig. 1B and D, Arrow-1), however, unexpectedly, there was also staining for IGFBP-1 observed in extravillous trophoblast cells (Fig. 2A–D, Arrow-2) possibly due to secreted IGFBP-1. No significant IGFBP-1 staining was observed in the villous trophoblasts or in negative controls (without any primary antibody or with pre-immune serum, not shown). IGFBP-1 was also largely absent in the cells of fetal origin, such as the fetal capillary endothelium, therefore, we concluded that the expression of IGFBP-1 was characteristically limited to the basal plate region of the decidua. Utilizing GA-matched AGA and IUGR

placental samples, the relative expression of IGFBP-1 in decidual cells, shown in Fig. 2, indicates relatively more abundant IGFBP-1 expression in IUGR (Fig. 1B and D) compared with AGA placenta (Fig. 1A and C).

IGFBP-1 Expression in Decidual Mesenchymal Cells Is Relatively Higher in IUGR Compared with AGA

Next, to quantify IGFBP-1 expression only in a subpopulation of truly decidualized mesenchymal cells of the placenta, we utilized a dual immunofluorescence approach combined with Image Pro software analysis. IGFBP-1 expression (merged yellow, Fig. 3A; Vimentin, pseudo-green/Alexa 660, Fig. 3B; and IGFBP-1, pseudo-red/Alexa 568, Fig. 3C) was assessed in a subpopulation of truly decidualized mesenchymal cells (Fig. 3A–L). Based on Image Pro software analysis as described in Materials and Methods and in flowchart (Fig. 2 and Supplemental Fig. 1), IGFBP-1 channel (Alexa 568, Fig. 3D and H and grayscale, Fig. 3I and J) shows the expression of IGFBP-1 within the outlines created in the vimentin channel (Alexa 660). The underlying IGFBP-1 signals cropped from the image (Fig. 3I and J) and recreated are shown in Fig. 3K and L in IUGR and AGA samples, respectively. By clearly isolating the signals within the vimentin positive cells, exclusive of overall background signals, overall cell-sorted images show enhanced IGFBP-1 signal intensity in the IUGR (Fig. 3L) versus AGA (Fig. 3K) likely to be in decidua. Accounting for IGFBP-1 only in the subpopulation of decidualized mesenchymal cells when they were removed from surrounding cells/tissue, we minimized the potential for false positive results. Furthermore, exclusion of primary antibody in the negative controls showed that the signal differences between the IUGR and AGA were highly specific to IGFBP-1 and were not due to autofluorescence or nonspecific binding of secondary antibodies (Supplemental Fig. 2).

IGFBP-1 Phosphorylation at Ser169, Ser119 and Ser101 in Decidual Mesenchymal Cells Is Markedly Enhanced in IUGR

Similarly, using the same methodology as used with Image Pro based software analysis for total IGFBP-1 (Figs. 2 and 3), we next evaluated IGFBP-1 phosphorylation (Alexa 568) at Ser169 (Fig. 4A–H), Ser119 (Fig. 5A–I) and Ser101 (Fig. 6A–I) within the vimentin positive (Alexa 660) subpopulation of decidualized mesenchymal cells in IUGR and AGA placenta. Phosphorylated IGFBP-1 channel (Alexa 568;

pseudo-red, Figs. 4–6, D and H) and the corresponding grayscale images (Figs. 4–6, I and J) indicate IGFBP-1 phosphorylation within the outlines created in the vimentin channel (Alexa 660). The underlying IGFBP-1 phosphorylation (Ser169, Ser119, and Ser101) signals cropped from the respective images and recreated are shown in Figs. 4–6 (K and L). The data with overall cell-sorted images provide a better visual prospective on changes in IGFBP-1 phosphorylation at all three serine sites in IUGR compared with AGA relative to pseudo colored images. The expression was likely to be mainly in truly decidualized mesenchymal cells.

Relative Quantitation of Decidual IGFBP-1 and IGFBP-1 Phosphorylation at Ser169, 119, and 101 in IUGR

We then quantified the relative changes in IGFBP-1 expression and phosphorylation at the three different serine sites in decidual mesenchymal cells of IUGR and AGA placenta. Utilizing set thresholds, levels of total IGFBP-1 expression and IGFBP-1 phosphorylation at Ser169, Ser119, and Ser101 were quantified within the outlines (Figs. 3–6, I and J) and are depicted in Fig. 2F. Based on second binary threshold within the mesenchymal cell outlines, we measured the subpopulation of decidualized mesenchymal cells to collect data only from highly IGFBP-1 expressing cells as described earlier (Fig. 2F).

The average of intensity measurements from six representative images ($n=6$) per placental tissue from AGA and IUGR group ($n=5$ each) were used for statistical analysis. The intensity comparison of total IGFBP-1 within the vimentin positive decidual cell population between AGA and IUGR placenta ($n=5$) showed relatively higher expression of total IGFBP-1 in IUGR decidua (+85%; $p=0.0001$; Fig. 7A) compared with GA-matched AGA decidua. Similarly, our data show relative IGFBP-1 phosphorylation in IUGR was markedly greater at Ser169 (+100%; $p=0.0021$) compared with AGA (Fig. 7B). Phosphorylation was also increased at Ser119 (+60%; $p=0.0064$; Fig. 7C) followed by Ser101 (+40%) compared with AGA (Fig. 7D). By measuring IGFBP-1 phosphoisoforms only in the specific decidual cell types, particularly in the heterogeneous cell population of the basal plate region, we have provided novel information to show that IGFBP-1 phosphorylation at Ser169 (Fig. 7B) comparative to the other two phosphorylation sites was relatively greater in IUGR versus AGA placenta.

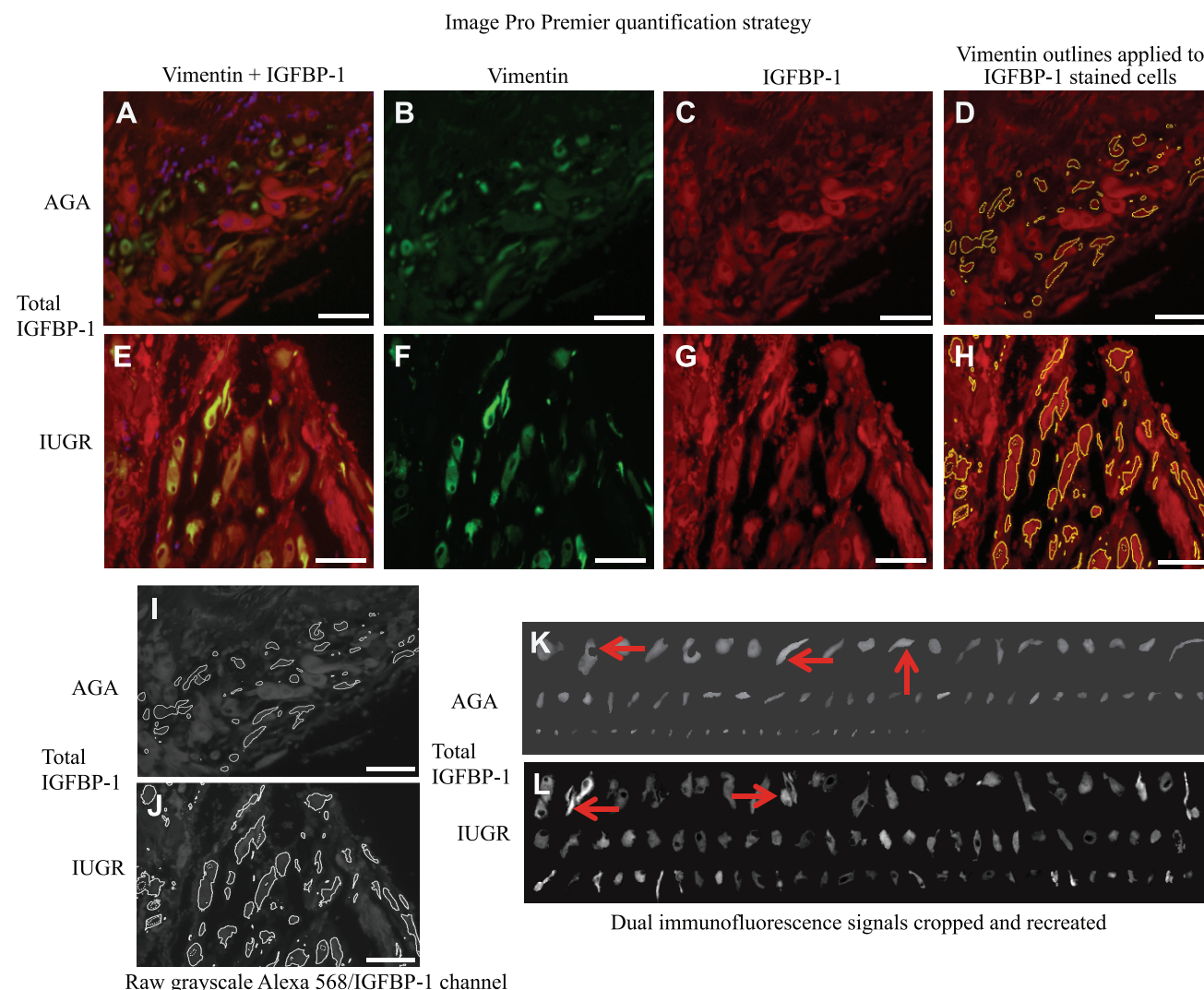


Figure 3. Relative dual immunofluorescence detection of total IGFBP-1 levels in AGA and IUGR placental tissues. Representative dual immunofluorescence IHC images of merged channels with IGFBP-1 (pseudo-red), vimentin (pseudo-green), and nuclei/DAPI (blue; A and E). Vimentin (pseudo-green, Alexa 660; B and F), IGFBP-1 (pseudo-red, Alexa 568; C and G). Cell outlines of vimentin positive cells applied to IGFBP-1 channel (Alexa 568; D and H). Alexa 568 image (D and H) also shown in grayscale for better viewing (I and J). Utilizing set thresholds, IGFBP-1 expression was then quantified within cell outlines (from I and J). Cell outlines were converted into multicell ROIs and applied onto the raw channel. A cell-sorted image was created to illustrate the intensity differences in signal between the IUGR and AGA (K and L). A few high IGFBP-1 expressing cells shown by red arrows, representative of the subpopulation of truly decidualized cells. IUGR pregnancies were noted to have higher expression of IGFBP-1 within the decidua of placental tissues compared with GA-matched AGA placenta ($n=5$ each). Scale bar = 50 μm . Abbreviations: IGFBP-1, insulin-like growth factor binding protein-1; AGA, appropriate for gestational age; IUGR, intrauterine growth restriction; IHC, immunohistochemistry; DAPI, 4',6-Diamidino-2-Phenylindole, Dihydrochloride; ROI, region of interest; GA, gestational age.

Discussion

To the best of our knowledge, this is the first study reporting that IGFBP-1 phosphorylation at Ser169 and Ser119 is markedly increased in the subpopulation of decidualized mesenchymal cells in IUGR placenta compared with GA-matched AGA. Given the well-established pronounced increase in IGF-1 affinity associated with

increased IGFBP-1 phosphorylation,²³ we speculate that decidual IGFBP-1 hyperphosphorylation reduces IGF-1 bioactivity within the local environment of the placenta,⁵ restricting placental growth and function, which may contribute to reduced fetal growth. In light of these findings, it will be important to study the signaling mechanisms that modulate decidual IGFBP-1 phosphorylation in IUGR, which are currently unclear.

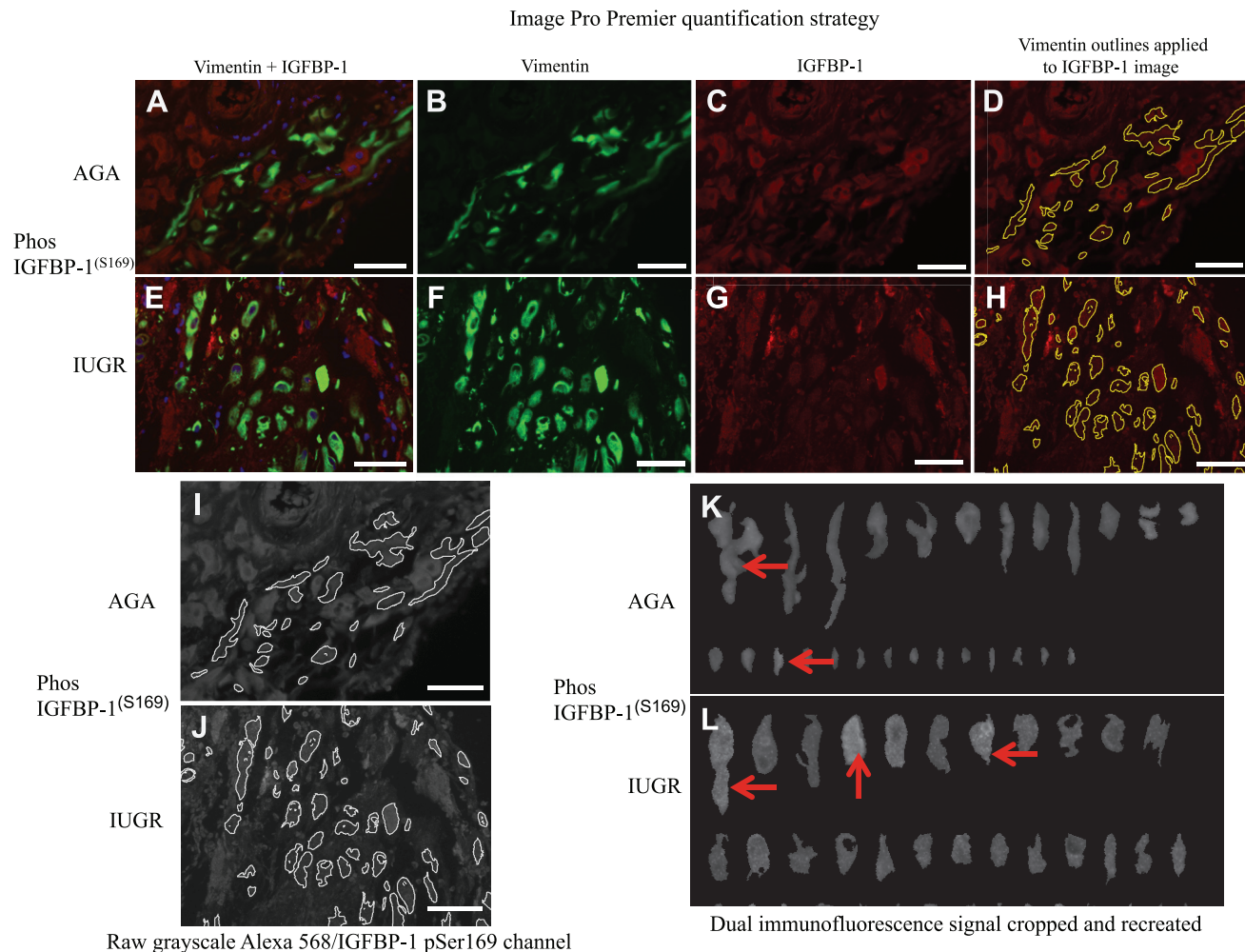


Figure 4. Relative dual immunofluorescence detection of phosphorylated IGFBP-1 (pSer169) in AGA and IUGR placenta tissues. Representative dual immunofluorescence IHC images of merged channels of phosphorylated IGFBP-1 (pSer169; pseudo-red), vimentin (pseudo-green), and nuclei/DAPI (blue; A and E). Vimentin (pseudo-green, Alexa 660; B and F), IGFBP-1 (pseudo-red, Alexa 568; C and G). Cell outlines of vimentin positive cells applied to IGFBP-1 channel (D and H). Alexa 568 image (D and H) also shown in grayscale for better viewing (I and J). Utilizing set thresholds, IGFBP-1 (pSer169) expression was then quantified within cell outlines (from I and J). Cell outlines were converted into multicell ROIs and applied onto the raw channel. A cell-sorted image was created to illustrate the intensity differences in signal between the IUGR and AGA (K and L). A few high phosphorylated IGFBP-1 (pSer169) expressing cells shown by red arrows (K and L). IUGR placental tissues exhibited a relatively higher IGFBP-1 phosphorylation (pSer169) compared with GA-matched AGA samples ($n=5$ each). Scale bar = 50 μ m. Abbreviations: IGFBP-1, insulin-like growth factor binding protein-1; AGA, appropriate for gestational age; IUGR, intrauterine growth restriction; IHC, immunohistochemistry; DAPI, 4',6-Diamidino-2-Phenylindole, Dihydrochloride; ROI, region of interest; GA, gestational age.

The small sample size represents a limitation of the current study. Nevertheless, even with a limited number of cases, these data corroborate our recent findings from decidualized HIESC linking decreased nutrient/oxygen levels to increased IGFBP-1 phosphorylation which are consistent with our clinical samples.¹⁸ The outcome of this study was based on our overall sample selection that ensured a very well controlled study group mainly based on the severity of IUGR. Another limitation of the study is that we examined the status of IGFBP-1 phosphorylation singly at

Ser101, 119, and 169, with our existing phospho-site antibodies. Considering that in our *in vitro* study, multiple reaction monitoring mass spectrometry (MRM-MS) allowed us to discover dually phosphorylated sites in decidualized HIESCs, it is therefore likely that combined pSer98+pSer101 and/or pSer174+pSer169 residues such as in HIESCs,¹⁸ may be affected clinically in IUGR with more severe consequences to fetal growth *in vivo*. Furthermore, IGFBP-1 is one of the few validated markers that can selectively identify decidualized cells from among the mixed cell

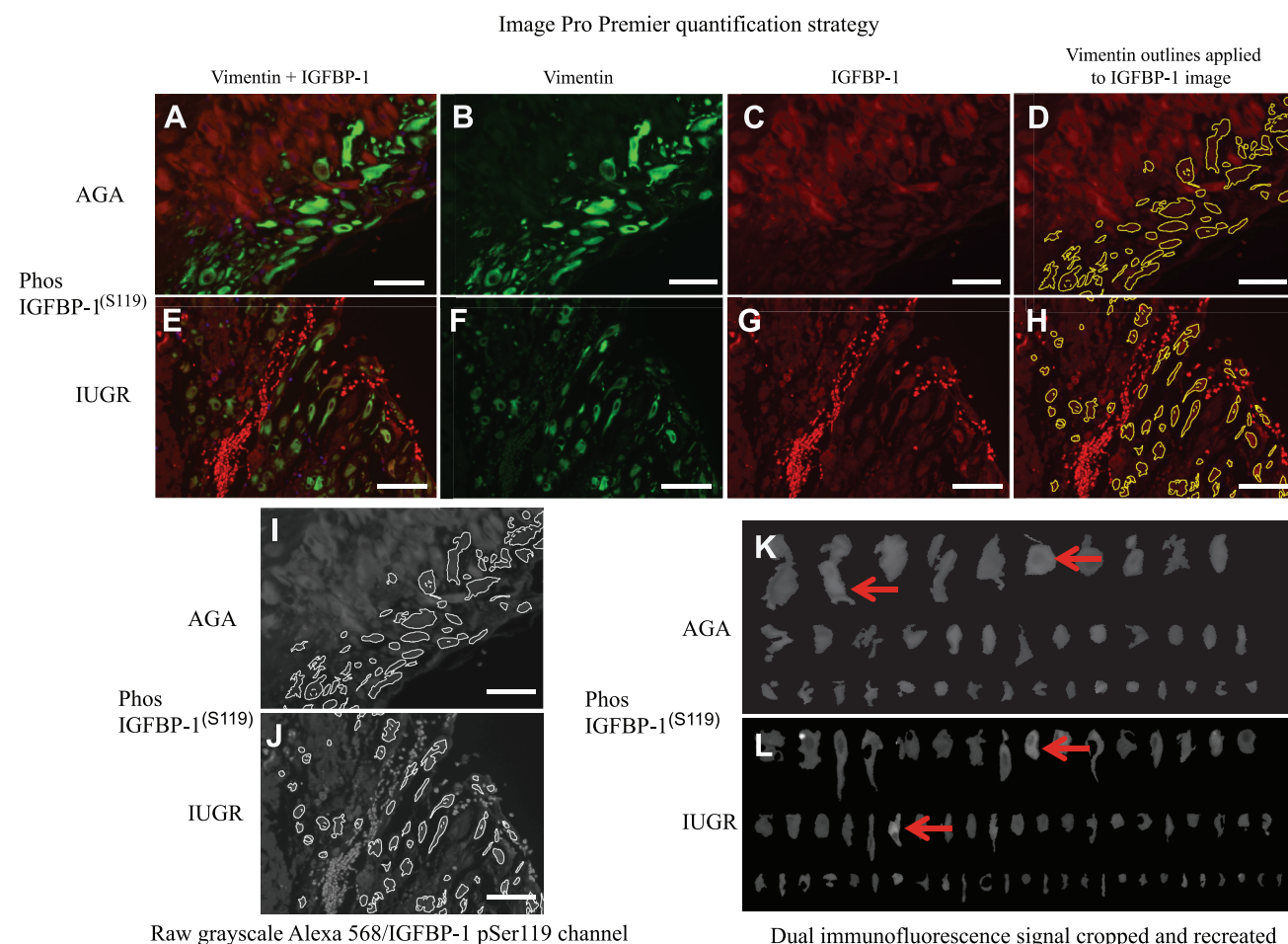


Figure 5. Relative dual immunofluorescence detection and quantitative analysis of phosphorylated IGFBP-1 (pSer119) in AGA and IUGR placenta tissues. Representative dual immunofluorescence IHC images of merged channels of phosphorylated IGFBP-1 (pSer119; pseudo-red), vimentin (pseudo-green), and nuclei/DAPI (blue; A and E). Vimentin (pseudo-green, Alexa 660; B and F), IGFBP-1 (pseudo-red, Alexa 568; C and G). Cell outlines of vimentin positive cells applied to IGFBP-1 channel (D and H). Alexa 568 image (D and H) also shown in grayscale for better viewing (I and J). Utilizing set thresholds, IGFBP-1 phosphorylation (pSer119) was then quantified within cell outlines (from I and J). Cell outlines were converted into multicell ROIs and applied onto the raw channel. A cell-sorted image was created to illustrate the intensity differences in signal between the IUGR and AGA (K and L). A few high expressing phosphorylated IGFBP-1 (pSer119) in IUGR placental tissues exhibited a relatively higher IGFBP-1 phosphorylation (pSer119) compared with GA-matched AGA samples ($n=5$ each). Scale bar = 50 μ m. Abbreviations: IGFBP-1, insulin-like growth factor binding protein-1; AGA, appropriate for gestational age; IUGR, intrauterine growth restriction; IHC, immunohistochemistry; DAPI, 4',6-Diamidino-2-Phenylindole, Dihydrochloride; ROI, region of interest; GA, gestational age.

population in the BPD region.¹⁶ IGFBP-1 staining in our tissues was observed also in adjacent extravillous trophoblast cells of the placenta (Fig. 1B, Arrow-2), which may be due to secretory nature of the protein but needs further explanation.

We have previously reported relative quantitation of IGFBP-1 phosphorylation in the liver of the IUGR baboon fetus using western blot and our custom phospho-site-specific antibodies.¹³ Here, to quantitate decidual IGFBP-1 phosphorylation in IUGR, an IHC approach was necessary to characterize the subpopulation of decidual cells within the mixed cell population

in the BPD, to limit our data to truly decidualized cells. Our unique image analysis strategy, combined with Image Pro software-based sensitive quantitation proved vital to precisely assess changes in IGFBP-1 phosphoisoforms specifically localized in the maternal decidualized mesenchymal cells of the BPD¹⁵ in IUGR compared with AGA not been studied earlier.

Decidualization is characterized by enhanced production of IGFBP-1 along with prolactin (PRL), and the forkhead transcriptional factor FOXO1.^{24–26} Furthermore, vimentin, desmin, alpha-2-macroglobulin are markers for mesenchymal-derived cells widely used for

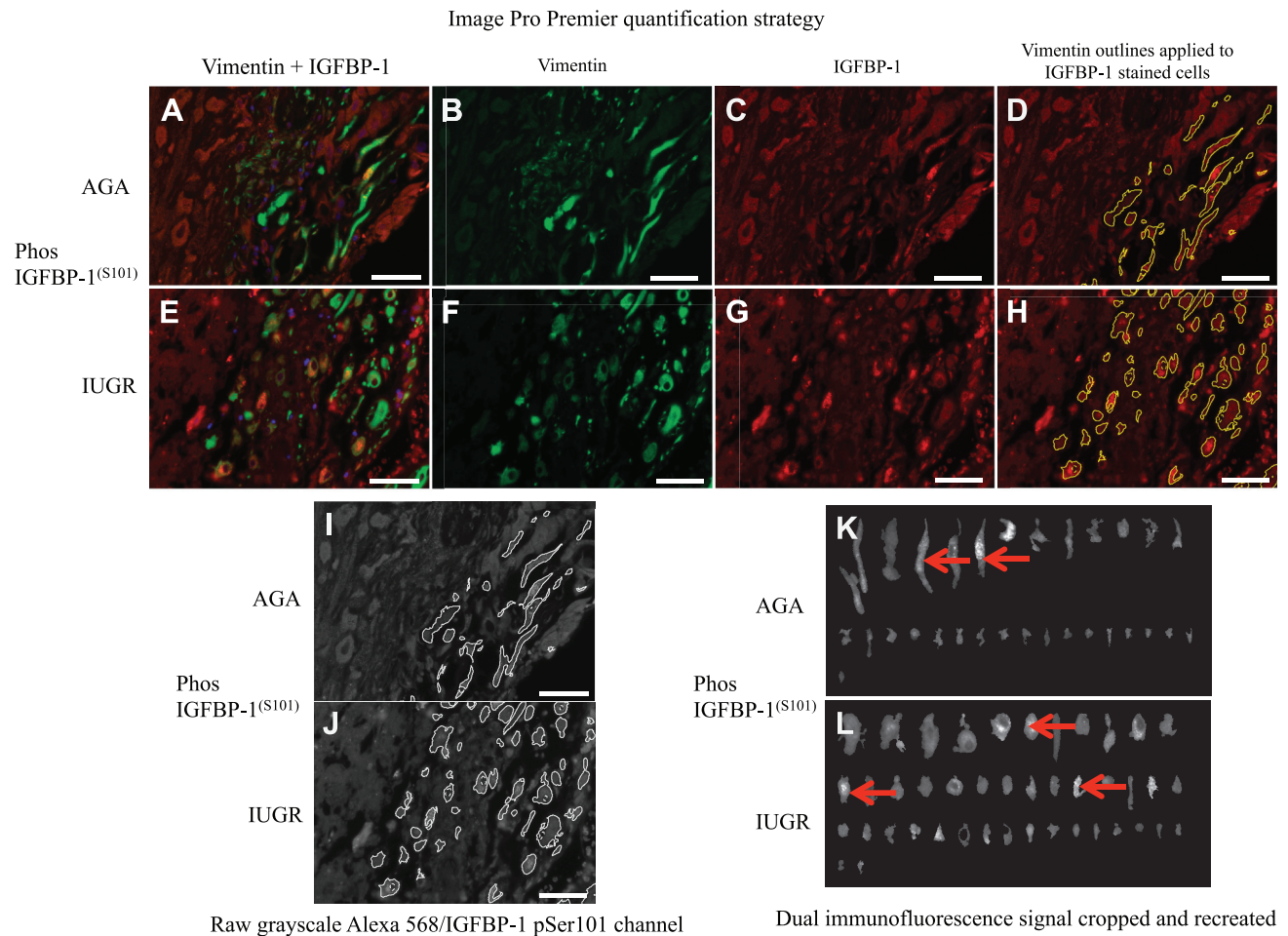


Figure 6. Relative dual immunofluorescence detection and quantitative analysis of phosphorylated IGFBP-1 (pSer101) in AGA and IUGR placenta tissues. Representative dual immunofluorescence IHC images of merged channels of phosphorylated IGFBP-1 (pSer101; pseudo-red), vimentin (pseudo-green), and nuclei/DAPI (blue; A and E). Vimentin (pseudo-green, Alexa 660; B and F), IGFBP-1 (pseudo-red, Alexa 568; C and G). Cell outlines of vimentin positive cells applied to IGFBP-1 channel (D and H). Alexa 568 image (D and H) also shown in grayscale for better viewing (I and J). Utilizing set thresholds, IGFBP-1 phosphorylation (pSer101) was then quantified within cell outlines (from I and J). Cell outlines were converted into multicell ROIs and applied onto the raw channel. A cell-sorted image was created to illustrate the intensity differences in signal between the IUGR and AGA (K and L). A few high expressing phosphorylated IGFBP-1 (pSer101) cells shown by red arrows. IUGR placental tissues exhibited a relatively higher IGFBP-1 phosphorylation (pSer169) compared with GA-matched AGA samples ($n=5$ each). Scale bar = 50 μm . Abbreviations: IGFBP-1, insulin-like growth factor binding protein-1; AGA, appropriate for gestational age; IUGR, intrauterine growth restriction; IHC, immunohistochemistry; DAPI, 4',6-Diamidino-2-Phenylindole, Dihydrochloride; ROI, region of interest; GA, gestational age.

characterizing mesenchymal-derived and decidual cells.²⁷ These proteins however, also represent other mesenchymal cell types, for example, fibroblasts.²⁷ IGFBP-1 is one of the few validated markers to selectively identify decidualized cells from among the mixed cell population in the BPD region.¹⁶ Therefore, to distinguish decidualized cells from undecidualized, vimentin positive “truly decidualized cells,” although there was potential for some bias, we used IGFBP-1 itself and performed the present study to isolate IGFBP-1 specifically in decidual cells versus whole, multicellular BPD region.

In addition, we showed here that increases in decidual IGFBP-1 phosphorylation in parallel with total IGFBP-1, which is in agreement with that we reported previously.¹⁴ We have earlier demonstrated that despite the unchanged phospho/total IGFBP-1 ratio, the hyperphosphorylation of IGFBP-1 due to hypoxia in cultured cells caused ~300-fold greater affinity for IGF-1 relative to the total IGFBP-1 in normal condition.¹⁴ Currently it is not known whether decidual IGFBP-1 hyperphosphorylation causes significant effects on IGF-1 affinity and/or bioavailability in human IUGR. The data from our current study nevertheless

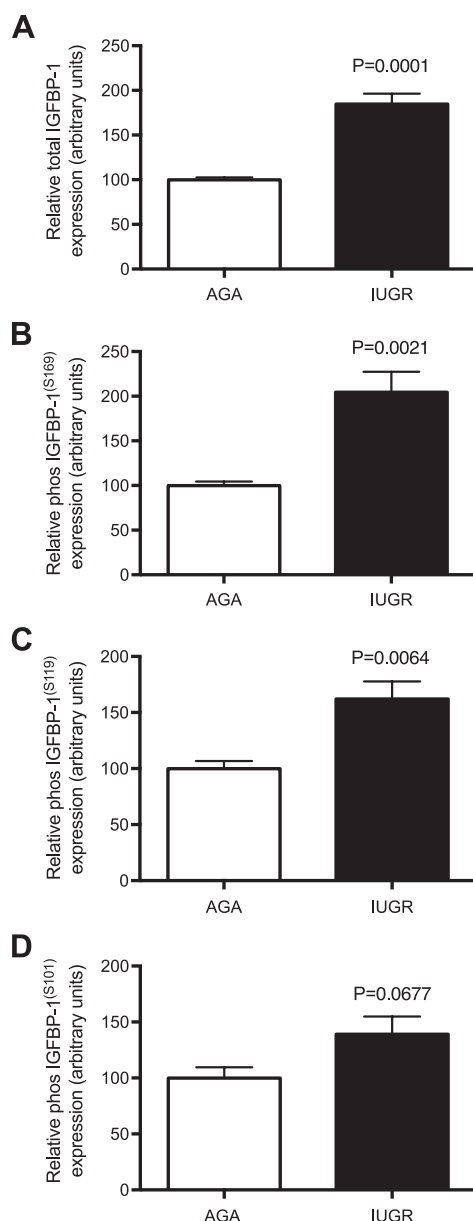


Figure 7. Quantitative analysis of the relative expression of decidual total IGFBP-1 and phosphorylated IGFBP-1 in AGA and IUGR placental tissues. Utilizing set thresholds, IGFBP-1 expression and phosphorylation was quantified within the white outlines shown in grayscale in Figs. 3 to 6, panels I and J in AGA and IUGR subjects. IUGR group was noted to have higher expression of total IGFBP-1 (A); phosphorylated IGFBP-1, pSer169 (B); phosphorylated IGFBP-1, pSer119 (C) and phosphorylated IGFBP-1, pSer101 (D) within the decidua of placental tissues compared with GA-matched AGA placenta ($n=5$ each). Values are given as means \pm SEM. $p \leq 0.05$ versus control as per unpaired Student's *t*-test. Abbreviations: IGFBP-1, insulin-like growth factor binding protein-1; AGA, appropriate for gestational age; IUGR, intrauterine growth restriction; GA, gestational age.

suggest that the predominant changes in IGF-1 affinity/bioavailability in decidua may not be due to levels of

total IGFBP-1 or total IGFBP-1 phosphoisoforms but because of combined effects of sites and degree of phosphorylation, which warrants further investigation.

The decidua constitutes the major source for maternal circulating IGFBP-1 in pregnancy.⁵ Locally in the placental barrier, IGFBP-1 inhibits trophoblast invasion both directly²⁸ and indirectly by sequestering IGF-1, a potent stimulator of trophoblast invasion.²⁹ Because maternal IGF-1 is a powerful positive regulator of placental function, changes in decidual IGFBP-1 secretion and phosphorylation may play a pivotal role in the development of IUGR. However, the underlying mechanisms remain elusive. Novel data from the current study will help us fill this significant gap in knowledge and allow testing our hypothesis that decidual nutrient sensing, constitutes a critical link between placental insufficiency and IUGR by regulating IGFBP-1 secretion and phosphorylation, which modulates maternal and local IGF-1 bioavailability and therefore placental function.

Furthermore, increased decidual IGFBP-1 phosphorylation may be a possible contributor to the elevated maternal circulating phosphorylated IGFBP-1 in IUGR. On that basis, the current study provides a strong rationale to examine early pregnancy maternal plasma to determine the role of specific IGFBP-1 phosphoisoforms in the prediction of IUGR. This could be used to improve the clinical management of these patients.

In summary, although the number of samples was limited, in the current study, we performed image analysis of placenta samples from IUGR and GA-matched AGA. This strategy enabled us to gain convincing novel data showing relatively increased site-specific IGFBP-1 phosphorylation in the subpopulation of decidualized, mesenchymal cells in IUGR versus AGA. It is expected that the relative abundance of IGFBP-1 hyperphosphorylation at the maternal-fetal interface may be inhibitory to the interaction of IGF-1 with its receptor. These data suggest that unique sites phosphorylated on IGFBP-1 may be important for regulating cellular growth and development by more potently binding IGF-1 and inhibiting its biological action,¹⁴ as well as limiting trophoblast invasion and migration.³

Acknowledgments

The authors thank the trainees Mr. Jiho Hong, Carl Reid, and Manthan Dhruv, who have contributed to the study as part of their undergraduate training program. We thank Biotron Integrated Microscopy facility, University of Western Ontario, in aiding for dual immunofluorescent image acquisition and analyses. We are thankful to Mr. Randy Bugdale for his graphic arts contribution in Fig. 2, and Dr. Mike Miller for review of the statistical analyses.

Competing Interests

The author(s) declared no potential conflicts of interest with respect to the research, authorship, and/or publication of this article.

Author Contributions

KN guided the immunofluorescence experiments and selected appropriate antibodies, reagents, and imaging parameters. SSS performed the experiments, captured the images, and analyzed the results. SSS and KN performed image analysis and contributed to interpretation of data. MBG and TJ made contributions to the conception and design of the experiments. All authors contributed to the writing of the paper and approved the final version of the manuscript.

Funding

The author(s) disclosed receipt of the following financial support for the research, authorship, and/or publication of this article: This work was supported by grants from the National Institute of Health (R01HD089980) to MBG and TJ and in part by the Lawson Health Research Institute and Children's Health Research Institute, Canada to MBG and RG.

ORCID iD

MB Gupta  <https://orcid.org/0000-0001-9197-0341>

Literature Cited

1. Brodsky D, Christou H. Current concepts in intra-uterine growth restriction. *J Intensive Care Med*. 2004;19(6):307–19. doi:10.1177/0885066604269663.
2. Barker DJ, Osmond C, Golding J, Kuh D, Wadsworth ME. Growth in utero, blood pressure in childhood and adult life, and mortality from cardiovascular disease. *BMJ*. 1989;298(6673):564–7.
3. Jansson T, Powell TL. Role of placental nutrient sensing in developmental programming. *Clin Obstet Gynecol*. 2013;56(3):591–601. doi:10.1097/GRF.0b013e3182993a2e.
4. Fowler DJ, Nicolaidis KH, Miell JP. Insulin-like growth factor binding protein-1 (IGFBP-1): a multifunctional role in the human female reproductive tract. *Hum Reprod Update*. 2000;6(5):495–504.
5. Martina NA, Kim E, Chitkara U, Wathen NC, Chard T, Giudice LC. Gestational age-dependent expression of insulin-like growth factor-binding protein-1 (IGFBP-1) phosphoisoforms in human extraembryonic cavities, maternal serum, and decidua suggests decidua as the primary source of IGFBP-1 in these fluids during early pregnancy. *J Clin Endocrinol Metab*. 1997;82(6):1894–8.
6. Rutanen EM, Bohn H, Seppala M. Radioimmunoassay of placental protein 12: levels in amniotic fluid, cord blood, and serum of healthy adults, pregnant women, and patients with trophoblastic disease. *Am J Obstet Gynecol*. 1982;144(4):460–3.
7. Popovici RM, Lu M, Bhatia S, Faessen GH, Giaccia AJ, Giudice LC. Hypoxia regulates insulin-like growth factor-binding protein 1 in human fetal hepatocytes in primary culture: suggestive molecular mechanisms for in utero fetal growth restriction caused by uteroplacental insufficiency. *J Clin Endocrinol Metab*. 2001;86(6):2653–9. doi:10.1210/jcem.86.6.7526.
8. Jones JI, Busby WH Jr, Wright G, Clemmons DR. Human IGFBP-1 is phosphorylated on 3 serine residues: effects of site-directed mutagenesis of the major phosphoserine. *Growth Regul*. 1993;3(1):37–40.
9. Jones JI, Busby WH Jr, Wright G, Smith CE, Kimack NM, Clemmons DR. Identification of the sites of phosphorylation in insulin-like growth factor binding protein-1. Regulation of its affinity by phosphorylation of serine 101. *J Biol Chem*. 1993;268(2):1125–31.
10. Coverley JA, Baxter RC. Phosphorylation of insulin-like growth factor binding proteins. *Mol Cell Endocrinol*. 1997;128(1–2):1–5.
11. Firth SM, Baxter RC. Cellular actions of the insulin-like growth factor binding proteins. *Endocr Rev*. 2002;23(6):824–54. doi:10.1210/er.2001-0033.
12. Gibson JM, Aplin JD, White A, Westwood M. Regulation of IGF bioavailability in pregnancy. *Mol Hum Reprod*. 2001;7(1):79–87.
13. Abu Shehab M, Damerill I, Shen T, Rosario FJ, Nijland M, Nathanielsz PW, Kamat A, Jansson T, Gupta MB. Liver mTOR controls IGF-I bioavailability by regulation of protein kinase CK2 and IGFBP-1 phosphorylation in fetal growth restriction. *Endocrinology*. 2014;155(4):1327–39. doi:10.1210/en.2013-1759.
14. Gupta MB. The role and regulation of IGFBP-1 phosphorylation in fetal growth restriction. *J Cell Commun Signal*. 2015;9(2):111–23. doi:10.1007/s12079-015-0266-x.
15. Han VK, Bassett N, Walton J, Challis JR. The expression of insulin-like growth factor (IGF) and IGF-binding protein (IGFBP) genes in the human placenta and membranes: evidence for IGF-IGFBP interactions at the feto-maternal interface. *J Clin Endocrinol Metab*. 1996;81(7):2680–93. doi:10.1210/jcem.81.7.8675597.
16. Giudice LC, Dsupin BA, Irwin JC. Steroid and peptide regulation of insulin-like growth factor-binding proteins secreted by human endometrial stromal cells is dependent on stromal differentiation. *J Clin Endocrinol Metab*. 1992;75(5):1235–41. doi:10.1210/jcem.75.5.1385468.
17. Crossey PA, Pillai CC, Miell JP. Altered placental development and intrauterine growth restriction in IGF binding protein-1 transgenic mice. *J Clin Invest*. 2002;110(3):411–8. doi:10.1172/jci10077.
18. Shehab MA, Biggar K, Singal SS, Nygard K, Shun-Cheng Li S, Jansson T, Gupta MB. Exposure of decidualized HIESC to low oxygen tension and leucine deprivation results in increased IGFBP-1 phosphorylation and reduced IGF-I bioactivity. *Mol Cell Endocrinol*. 2017;452:1–14. doi:10.1016/j.mce.2017.04.005.
19. Abu Shehab M, Khosravi J, Han VK, Shilton BH, Gupta MB. Site-specific IGFBP-1 hyper-phosphorylation in fetal growth restriction: clinical and functional relevance.

- J Proteome Res. 2010;9(4):1873–81. doi:10.1021/pr900987n.
20. Nissum M, Abu Shehab M, Sukop U, Khosravi JM, Wildgruber R, Eckerskorn C, et al. Functional and complementary phosphorylation state attributes of human insulin-like growth factor-binding protein-1 (IGFBP-1) isoforms resolved by free flow electrophoresis. *Mol Cell Proteomics*. 2009;8(6):1424–35. doi:10.1074/mcp.M800571-MCP200.
 21. Seferovic MD, Chen S, Pinto DM, Gupta MB. Altered liver secretion of vascular regulatory proteins in hypoxic pregnancies stimulate angiogenesis in vitro. *J Proteome Res*. 2011;10(4):1495–504. doi:10.1021/pr100879z.
 22. Seferovic MD, Gupta MB. Increased umbilical cord PAI-1 levels in placental insufficiency are associated with fetal hypoxia and angiogenesis. *Dis Markers*. 2016;2016:7124186. doi:10.1155/2016/7124186.
 23. Abu Shehab M, Iosef C, Wildgruber R, Sardana G, Gupta MB. Phosphorylation of IGFBP-1 at discrete sites elicits variable effects on IGF-I receptor autophosphorylation. *Endocrinology*. 2013;154(3):1130–43. doi:10.1210/en.2012-1962.
 24. Guzel E, Buchwalder L, Basar M, Kayisli U, Ocak N, Bozkurt I, Lockwood CJ, Schatz F. Effects of tibolone and its metabolites on prolactin and insulin-like growth factor binding protein-1 expression in human endometrial stromal cells. *Gynecol Endocrinol*. 2015;31(5):414–8. doi:10.3109/09513590.2015.1014788.
 25. Kusama K, Yoshie M, Tamura K, Kodaka Y, Hirata A, Sakurai T, Bai H, Imakawa K, Nishi H, Isaka K, Nagai T, Nagao T, Tachikawa E. Regulation of decidualization in human endometrial stromal cells through exchange protein directly activated by cyclic AMP (Epac). *Placenta*. 2013;34(3):212–21. doi:10.1016/j.placenta.2012.12.017.
 26. Brucker SY, Eisenbeis S, König J, Lamy M, Salker MS, Zeng N, Seeger H, Henes M, Schöller D, Schönfisch B, Staebler A, Taran FA, Wallwiener D, Rall K. Decidualization is impaired in endometrial stromal cells from uterine rudiments in Mayer-Rokitansky-Kuster-Hauser Syndrome. *Cell Physiol Biochem*. 2017;41(3):1083–97. doi:10.1159/000464116.
 27. Costa AF, Gomes SZ, Lorenzon-Ojea AR, Martucci M, Faria MR, Pinto Ddos S Jr, Oliveira SF, Ietta F, Paulesu L, Bevilacqua E. Macrophage migration inhibitory factor induces phosphorylation of Mdm2 mediated by phosphatidylinositol 3-kinase/Akt kinase: role of this pathway in decidual cell survival. *Placenta*. 2016;41:27–38. doi:10.1016/j.placenta.2016.03.001.
 28. Irwin JC, Giudice LC. Insulin-like growth factor binding protein-1 binds to placental cytotrophoblast alpha5beta1 integrin and inhibits cytotrophoblast invasion into decidualized endometrial stromal cultures. *Growth Horm IGF Res*. 1998;8(1):21–31.
 29. Lacey H, Haigh T, Westwood M, Aplin JD. Mesenchymally-derived insulin-like growth factor 1 provides a paracrine stimulus for trophoblast migration. *BMC Dev Biol*. 2002;2:5.